

Correspondence

The first World Cell Race

Paolo Maiuri<sup>1</sup>, Emmanuel Terriac<sup>1</sup>, Perrine Paul-Gilloteaux<sup>1</sup>, Timothée Vignaud<sup>2</sup>, Krista McNally<sup>3</sup>, James Onuffer<sup>3</sup>, Kurt Thorn<sup>3</sup>, Phuong A. Nguyen<sup>4</sup>, Nefeli Georgoulia<sup>4</sup>, Daniel Soong<sup>5</sup>, Asier Jayo<sup>5</sup>, Nina Beil<sup>6</sup>, Jürgen Beneke<sup>6</sup>, Joleen Chooi Hong Lim<sup>7</sup>, Chloe Pei-Ying Sim<sup>7</sup>, Yeh-Shiu Chu<sup>7</sup>, WCR participants<sup>8</sup>, Andrea Jiménez-Dalmaroni<sup>9</sup>, Jean-François Joanny<sup>9</sup>, Jean-Paul Thiery<sup>7</sup>, Holger Erfle<sup>6</sup>, Maddy Parsons<sup>5</sup>, Timothy J. Mitchison<sup>4</sup>, Wendell A. Lim<sup>3</sup>, Ana-Maria Lennon-Duménil<sup>10</sup>, Matthieu Piel<sup>1,\*</sup>, and Manuel Théry<sup>2,\*</sup>.

Motility is a common property of animal cells. Cell motility is required for embryogenesis [1], tissue morphogenesis [2] and the immune response [3] but is also involved in disease processes, such as metastasis of cancer cells [4]. Analysis of cell migration in native tissue *in vivo* has yet to be fully explored, but motility can be relatively easily studied *in vitro* in isolated cells. Recent evidence suggests that cells plated *in vitro* on thin lines of adhesive proteins printed onto culture dishes can recapitulate many features of *in vivo* migration on collagen fibers [5,6]. However, even with controlled *in vitro* measurements, the characteristics of motility are diverse and are dependent on the cell type, origin and external cues. One objective of the first World Cell Race was to perform a large-scale comparison of motility across many different adherent cell types under standardized conditions. To achieve a diverse selection, we enlisted the help of many international laboratories, who submitted cells for analysis. The large-scale analysis, made feasible by this competition-oriented collaboration, demonstrated that higher cell speed correlates with the persistence of movement in the same direction irrespective of cell origin.

The race track consisted of 4 μm and 12 μm-wide fibronectin lines printed in multi-well glass-bottomed cell-culture wells (see Supplemental Experimental Procedures and Figure S1A in the Supplemental Information available online); 54 different cell types from various animals and tissues were provided by 47 laboratories. Genotypically, cells were wild type, transformed or genetically engineered (Table S1). The cells were distributed to six organizing laboratories (two in the USA, and one each in the UK,

France, Germany and Singapore), who prepared cell-culture stocks using the frozen samples received from participating laboratories and plated these onto the race tracks under identical culture conditions. Cells were allowed to adhere overnight and cell motility was recorded for 24 hours using an inverted video microscope (Figure 1B, Movie S1). Cell morphology (length, shape, symmetry, and nucleus position) varied greatly from one cell type to another (Figure 1A). Cell nuclei were

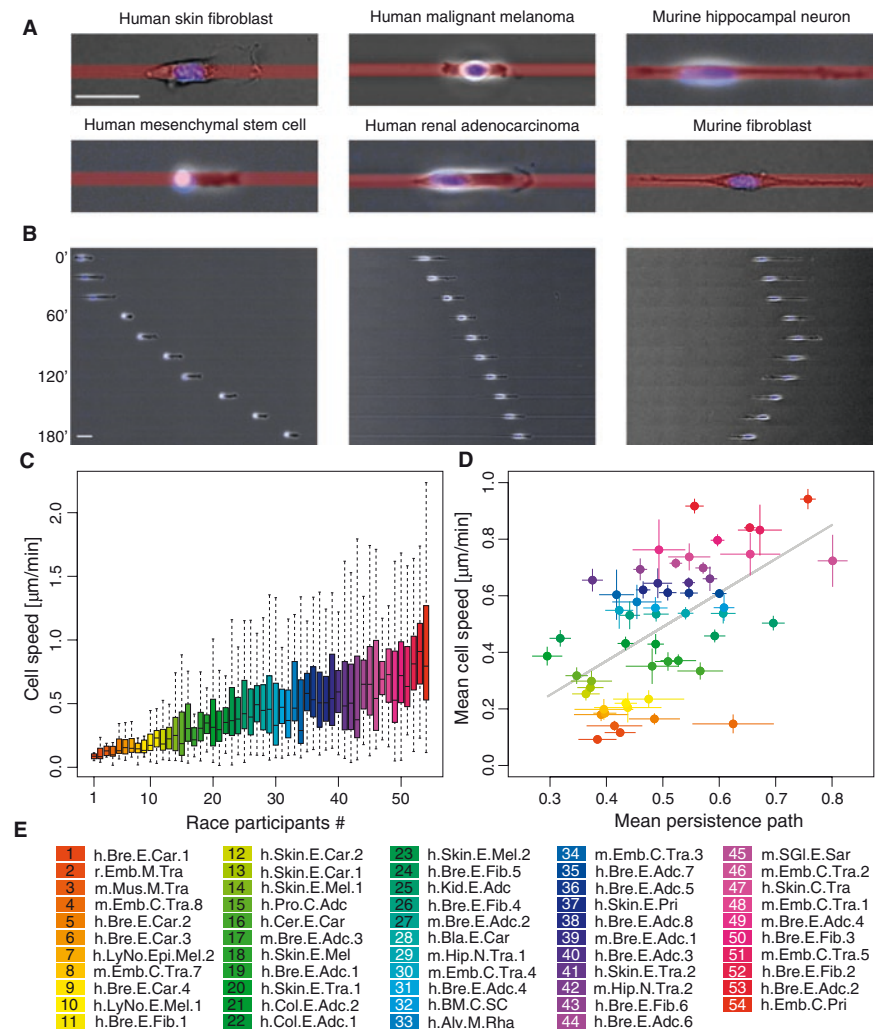


Figure 1. Cell speed and motion persistence on race tracks. (A) Images illustrating cell shape variability on micropatterned tracks. (B) Kymographs illustrating different types of cell motility. Scales bars represent 50 μm. (C) Cell speed distributions represented with quartile diagrams for all participants. (D) Mean cell speeds plotted versus mean persistence. Bars correspond to standard deviation. Pearson correlation coefficient of the linear fit is 0.58. All cells analyzed are listed and color coded. (E) Color-coded participating cell types list: cell type – organism.source. tissue.tumor. Organisms: human (h), mouse (m), rat (r). Sources: embryo (Emb), alveola (Alv), bladder (Blad), bone marrow (BM), breast (Bre), cervix (Cer), colon (Col), hippocampus (Hip), kidney (Kid), lymph node (LyNo), muscle (Mus), prostate (Pro), salivary glands (SGI), skin. Tissues: epithelial (E), connective (C), muscle (M), nervous (N). Tumors: transformed (Tra), adenocarcinoma (Adc), carcinoma (Car), fibroma (Fib), melanoma (Mel), primary (Pri), rhabdomyosarcoma (Rha), sarcoma (Sar), stem cells (SC).

stained by incubating live cells with 5 ng/ml Hoechst dye diluted in normal growth medium. Cell displacements were monitored every 10 minutes. Nuclei images were segmented and geometric centers were tracked with a global minimization algorithm in order to track automatically individual cell displacements (see Supplemental Experimental Procedures and Figure S1B). The motility of over 7,000 cells was compared, with an average of 130 cells analyzed per cell type. Detailed statistical analyses were used to characterize cell motility parameters for each cell type (see <http://www.worldcellrace.com/ResultFiles>).

The mean instantaneous speed of individual cells is computed by averaging the cell displacements between consecutive frames over time. The distribution of mean instantaneous speeds for each cell type was asymmetric (Figure 1C) and non-Gaussian (Figure S1C). Interestingly, we observed that a higher mean speed for a given cell type did not reflect a global shift of the speed distribution, but rather the spreading of the distribution due to the presence of faster moving cells (Figure 1C and Figure S1C). In order to identify the 2011 World Cell Race winner, only cells with an effective overall displacement of at least 350  $\mu\text{m}$  were considered. This cut-off was only reached by 26 of the 54 cell types. The highest migration speed was recorded at 5.2  $\mu\text{m}/\text{min}$  by a human embryonic mesenchymal stem cell (Movie S2).

Cell displacements on lines can be described by a 1D correlated random walk [7], simply derived from the 2D model, in which cells are more likely to move in the direction of the immediately preceding movement conserving their polarity. This can be quantified by a *persistence probability* ( $p$ ) for a cell to maintain its direction of motion and keep the same *front* and *rear*. For each cell type, we measured the number of cell steps between two motion reversals, i.e. the number of consecutive time intervals during which cells kept moving in the same direction (Figure S1E). To calculate  $p$ , histograms built from the number of cell steps, ~~ie the~~ **(AU: this correction to your proofs seems to be incomplete)** were fitted to the 1D correlated random walk theory (Figure S1D). A persistence path, defined as the ratio of the effective maximum

displacement to the actual trajectory length, was further calculated to obtain a macroscopic measure of  $p$  (Figure S1F). This ratio was strongly correlated with the persistence probability (Figure S1G). Persistence path distributions for the 54 cell types were typically non-Gaussian (Figure S1H). Strikingly, the overall mean speeds for all cell types correlated well with their mean persistence path (Figure 1D), implying that fast-moving cell-types (mean cell speed  $>0.7 \mu\text{m}/\text{min}$ ) displayed high mean persistence path ( $>0.5$ ). Cells moving rapidly, but only backwards and forwards, were not observed.

Given the large and diverse sample of cell types, this result may reveal a conserved mechanism that allows the coupling of the machinery controlling cell polarity (responsible for persistent oriented motion) to the one regulating instantaneous cell speed. Future experiments aimed at unraveling the associated molecular mechanisms shall now be performed.

Together, the results generated by the first World Cell Race highlight how scientific games involving large-scale experiments can lead to the identification of novel and relevant biological processes, which may otherwise escape observation.

#### Supplemental Information

Supplemental Information includes experimental procedures, one figure, one table and two movies and can be found with this article online at <http://dx.doi.org/10.1016/j.cub.2012.07.052>.

#### Acknowledgments

We thank all the participants who sent cells to the inaugural World Cell Race (listed in Table S1). We thank the Société de Biologie Cellulaire de France for its financial support and the American Society for Cell Biology for the organization of the session dedicated to the race during the 2011 annual meeting. We thank our industrial partners, Cytoo and Nikon Instruments, who provided the micropatterned substrates and the imaging platforms respectively.

P. Maiuri received a fellowship from the Fondation pour la Recherche Médicale, M. Parsons is funded by a Royal Society University Research Fellowship, H. Erfle and J. Beneke by the CellNetworks-Cluster of Excellence (EXC81), J. Onuffer, W.A. Lim and T.J. Mitchison by the NIH (PN2EY016546, GM23928), A. Lennon-Duménil and M. Piel by the ANR and Innabiosanté (09-PIRI-0027-PCVI and MICEMICO), M. Théry by the INCA (PLBIO-2011-141).

#### References

1. Keller, P.J., Schmidt, A.D., Wittbrodt, J., and Stelzer, E.H.K. (2008). Reconstruction of zebrafish early embryonic development by scanned light sheet microscopy. *Science* 322, 1065–1069.
2. Rembold, M., Loosli, F., Adams, R.J., and Wittbrodt, J. (2006). Individual cell migration serves as the driving force for optic vesicle evagination. *Science* 313, 1130–1134.
3. Faure-André, G., Vargas, P., Yuseff, M.-I., Heuzé, M., Diaz, J., Lankar, D., Steri, V., Manry, J., Hugues, S., and Vascotto, F., et al. (2008). Regulation of dendritic cell migration by CD74, the MHC class II-associated invariant chain. *Science* 322, 1705–1710.
4. Gligorijevic, B., Wyckoff, J., Yamaguchi, H., Wang, Y., Roussos, E.T., and Condeelis, J. (2012). N-WASP-mediated invadopodium formation is involved in intravasation and lung metastasis of mammary tumors. *J. Cell Sci.* 125, 724–734.
5. Pouthas, F., Girard, P., Lecaudey, V., Ly, T.B.N., Gilmour, D., Boulin, C., Pepperkok, R., and Reynaud, E.G. (2008). In migrating cells, the Golgi complex and the position of the centrosome depend on geometrical constraints of the substratum. *J. Cell Sci.* 121, 2406–2414.
6. Doyle, A.D., Wang, F.W., Matsumoto, K., and Yamada, K.M. (2009). One-dimensional topography underlies three-dimensional fibrillar cell migration. *J. Cell Biol.* 184, 481–490.
7. Codling, E.A., Plank, M.J., and Benhamou, S. (2008). Random walk models in biology. *J. R. Soc. Interface* 5, 813–834.

<sup>1</sup>Institut Curie, CNRS, UMR144, 75248, Paris, France. <sup>2</sup>Institut de Recherches en Sciences et Technologies pour le Vivant, CEA, UJF, CNRS, INRA, 38054, Grenoble, France.

<sup>3</sup>Department of Cellular and Molecular Pharmacology, UCSF, San Francisco, CA 94158, USA. <sup>4</sup>Harvard Medical School, Systems Biology, Boston, MA 02115, USA.

<sup>5</sup>Kings College London, SE1 1UL London, UK. <sup>6</sup>BioQuant, Heidelberg University, Germany. <sup>7</sup>Institute of Molecular and Cell Biology, A\*Star, Proteos, 138673, Singapore.

<sup>8</sup>World Wide, listed in Supplemental Information. <sup>9</sup>Institut Curie, CNRS, UMR168, 75248, Paris, France. <sup>10</sup>Institut Curie, INSERM, U639, 75248, Paris, France.

\*E-mail: [matthieu.piel@curie.fr](mailto:matthieu.piel@curie.fr), [manuel.thery@cea.fr](mailto:manuel.thery@cea.fr)